

SUPPORTING INFORMATION

ZIF-Derived CoP as Cocatalyst for Enhanced Photocatalytic H₂

Production Activity of g-C₃N₄

Xiao-Jun Sun,^{a,*} Dou-Dou Yang,^a Hong Dong,^{a,b} Xiang-Bin Meng,^a
Jing-Li Sheng,^a Xin Zhang,^a Jin-Zhi Wei^a and Feng-Ming Zhang^{a,*}

*a. Key Laboratory of Green Chemical Engineering and Technology of
College of Heilongjiang Province, College of Chemical and
Environmental Engineering, Harbin University of Science and
Technology, Harbin 150040, P. R. China.*

*b. Ministry of Education Key Laboratory of Engineer Dielectrics and Its
Application, College of Material Science and Engineering, Harbin
University of Science and Technology, Harbin 150040, P. R. China.*

**E-mail: zhangfm80@163.com. Fax: (+86) 451 8639 2713.*

Table of Contents

Characterization	S3
Photocatalytic hydrogen production	S3
Electrochemical characterization	S3
Computational details	S3
Figure S1-S3 Characterizations of ZIF-67	S4
Figure S4-S6 Characterizations of g-C ₃ N ₄	S5
Figure S7-S9 Characterizations of photocatalysts	S6
Figure S10-S13 Photocatalytic hydrogen production	S7-9
Table S1 Summary of various catalysts for photocatalytic H ₂ evolution	S10

Characterization

The characteristics of the materials were investigated by Fourier transform infrared (FTIR) spectra (Spectrum 100), X-ray powder diffraction (XRD) patterns (Bruker D8 X-ray diffractometer), scanning electron microscopy (SEM) micrographs (Hitachi S-4800), the transmission electron microscopy (TEM) experiment (JEM-2100 electron microscope), diffuse reflectance UV-vis spectroscopy techniques (Lambda 35 spectrometer), X-ray photoelectron spectroscopy (XPS) techniques (Kratos-AXIS ULTRA DLD apparatus), the photoluminescence (PL) spectra (SPEX Fluorolog-3 spectrofluorometer) and thermogravimetric analyses (TGA/SDTA851e).

Photocatalytic hydrogen production

Visible light driven H_2 evolution reactions were conducted in a closed gas circulation and evacuation system fitted with a top window Pyrex cell (CEAULIGHT CEL-SPH2N). Online gas chromatograph of GC112A with a TCD was used in the process to detect the evolution of gas. Make the system vacuumed for 0.5 h to remove the dissolved oxygen with vacuum bump. In a typical reaction, the photocatalyst (30 mg) was added in 50 ml of 10 vol% triethanolamine (TEOA) aqueous solution without H_2PtCl_6 after sonication for 20 min. Then the solution was irradiated with a 300 W Xe lamp equipped with an appropriate cut-off filter under vigorous stirring. Meanwhile, gas circulator was adopted and a cooling water jacket was disposed to keep the temperature of reactor at around 6 °C. Apparent quantum yield (AQY) was calculated by using the following formula: $AQY = (2 \times \text{the number of evolved hydrogen molecules}) / (\text{the number of incident photons}) \times 100\%$. To obtain the number of incident photons, the following calculations were done. The number of incident photons $N = P t \lambda / h c$. The t represents reaction time. Planck constant $h = 6.62606896 \times 10^{-34}$ J·s. Speed of light $c = 299792458$ m s⁻¹. The λ is the wavelength of incident light. Average radiation flux of incident light $P = E A_R$. The E represents the mean of irradiance measured by light power meter. Reactor light receiving area $A_R = \pi R^2$. The π is circumference ratio 3.1416. The R is the corresponding radius of light receiving area. Then, the number of incident photons can be obtained. Notably, wavelengths at 380, 420 and 450 nm were adopted and the corresponding apparent

quantum yields (AQY) were calculated.

Electrochemical characterization

The electrochemical impedance spectra (EIS), Mott-Schottky plot and photocurrent-time (I-T) profiles were recorded on the CHI660e by using three-electrode cells. 0.1 M Na₂SO₄ solutions, Ag/AgCl reference electrode, a Pt counter electrode and ITO glass substrate electrodes were adopted. The photocatalysts were fabricated onto ITO glass substrate electrodes via immersion in the mixed solution with ethanol suspension of photocatalyst.

Computational details

Geometry optimizations and electronic structure calculations for the periodic systems are based on density functional theory (DFT) methods implemented in the SIESTA package. The generalized gradient approximation (GGA) in the Perdue–Burke–Ernzerhof (PBE) form is used to treat the exchange–correlation potential, and the double-z polarization (DZP) basis sets are selected for the DFT calculations. A real-space grid with an equivalent energy cutoff of 150 Ry is adopted to expand the electron density for numerical integration. A vacuum layer greater than 10 Å is used so that interaction among periodic images can be neglected. All the atoms in the unit cell are fully relaxed with the force on each atom being less than 0.01 eV Å⁻¹ and the total energy changes being less than 0.0001 eV. The Brillouin zone is sampled at $1 \times 100 \times 100$ (x, y, and z directions, respectively) Monkhorst meshes for 2D structures.

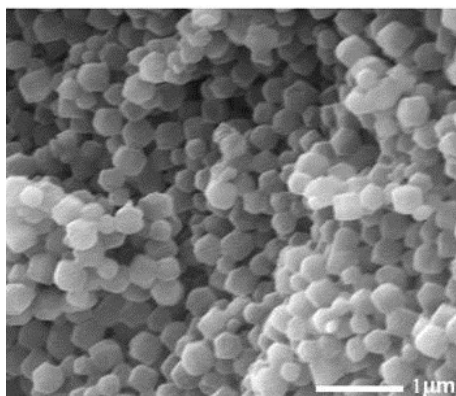


Fig. S1 SEM images of ZIF-67.

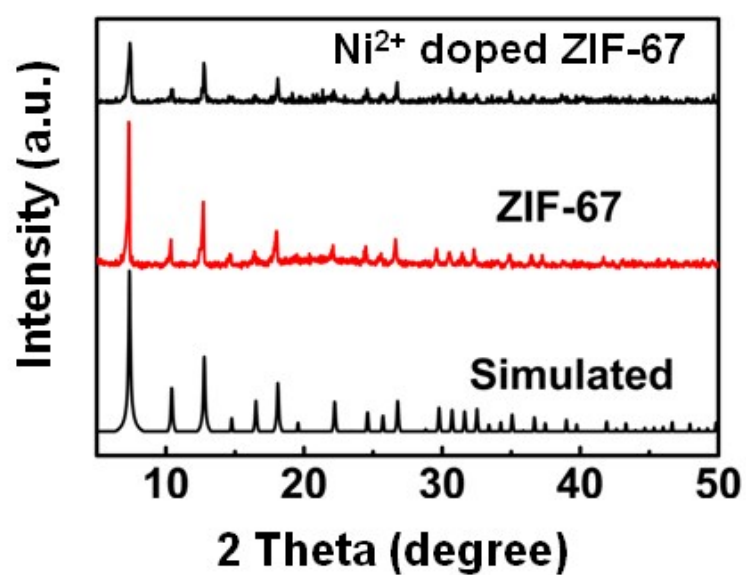


Fig. S2 XRD patterns of ZIF-67, Ni^{2+} doped ZIF-67 and the simulated sample.

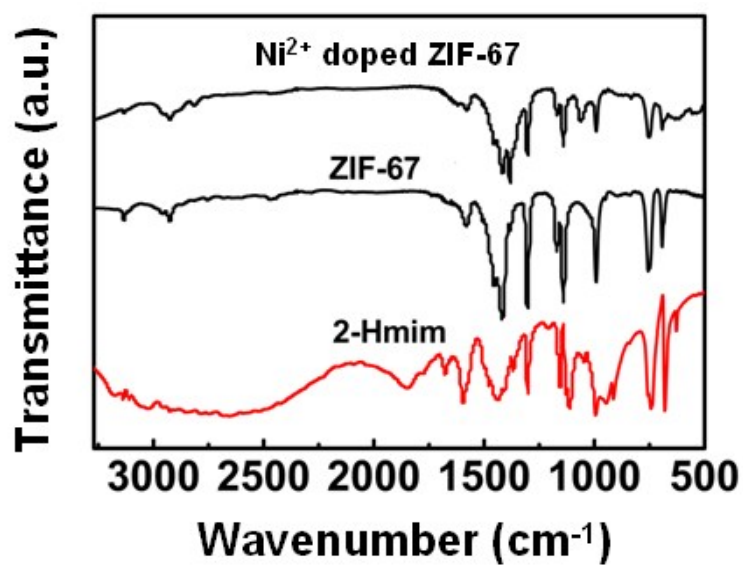


Fig. S3 FT-IR spectra of 2-Hmim (2-methylimidazole) and ZIF-67, Ni^{2+} doped ZIF-67.

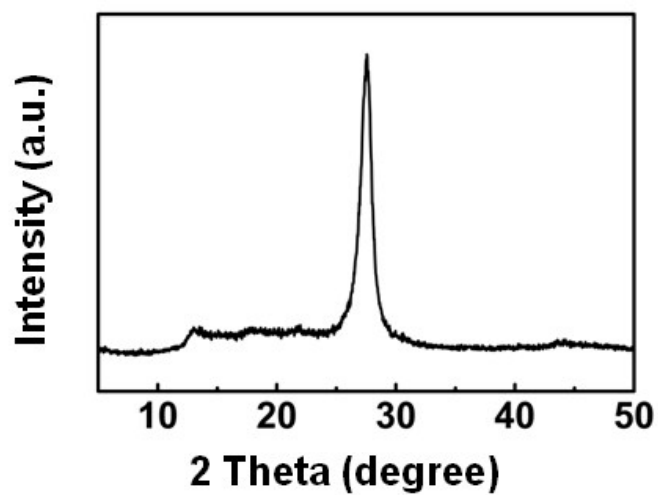


Fig. S4 XRD pattern of g-C₃N₄.

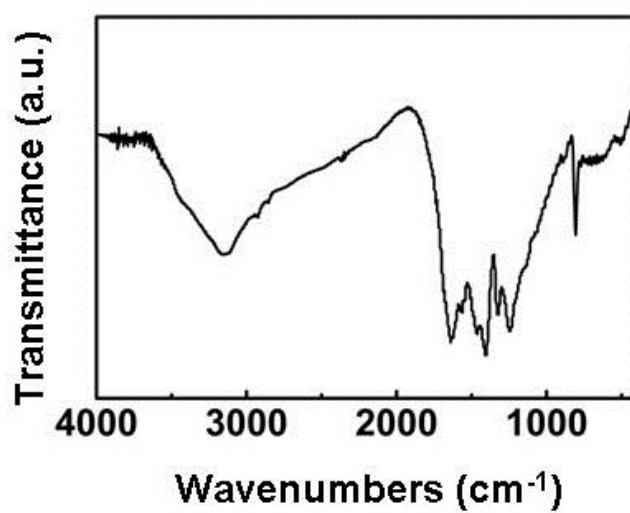


Fig. S5 FT-IR spectra of g-C₃N₄.

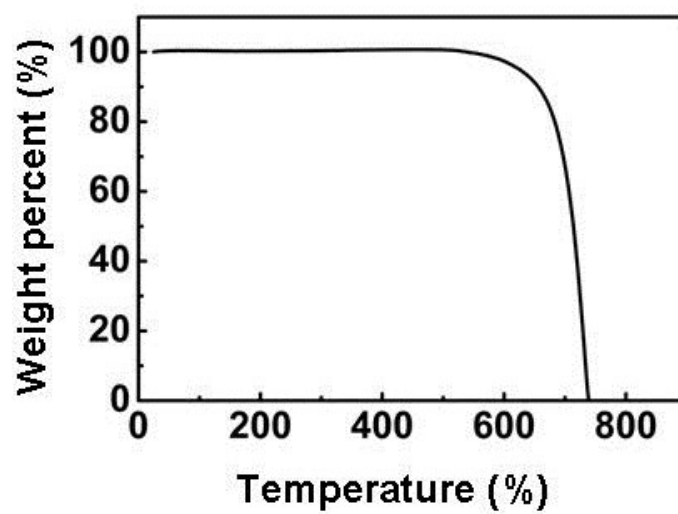


Fig. S6 TG curve of g-C₃N₄.

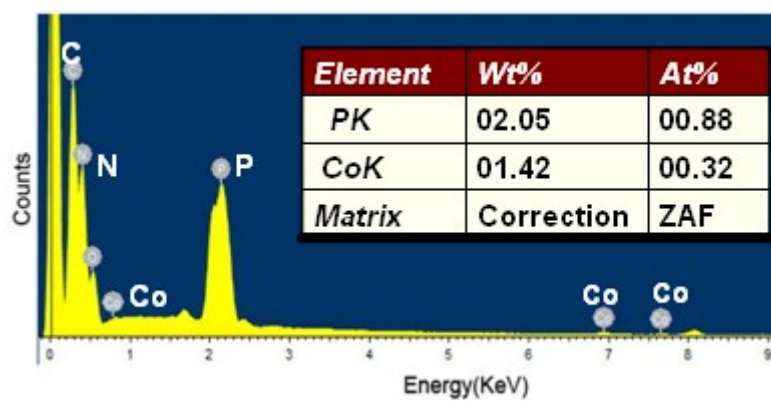


Fig.S7 EDS spectrum of CoP/g-C₃N₄-5.

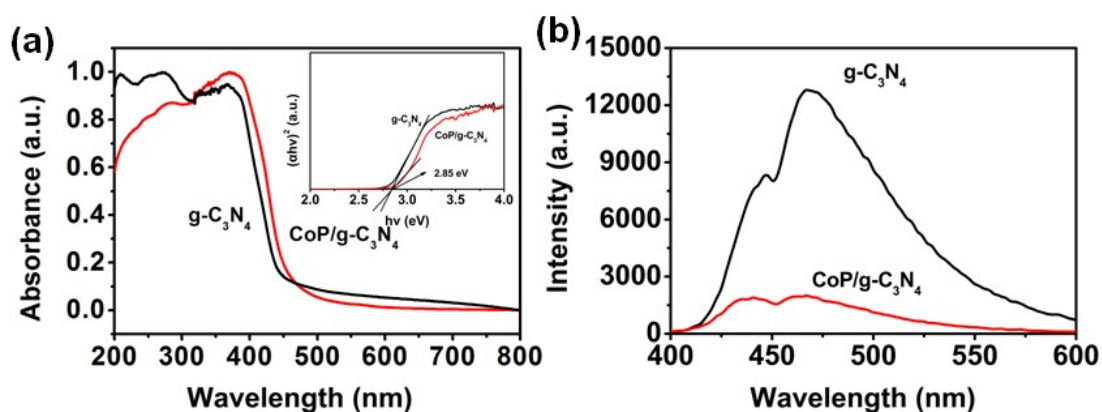


Fig. S8 (a) Diffuse reflectance UV-vis spectra of CoP/g-C₃N₄ and g-C₃N₄. (b) Photoluminescence spectra of as-prepared CoP/g-C₃N₄ and g-C₃N₄.

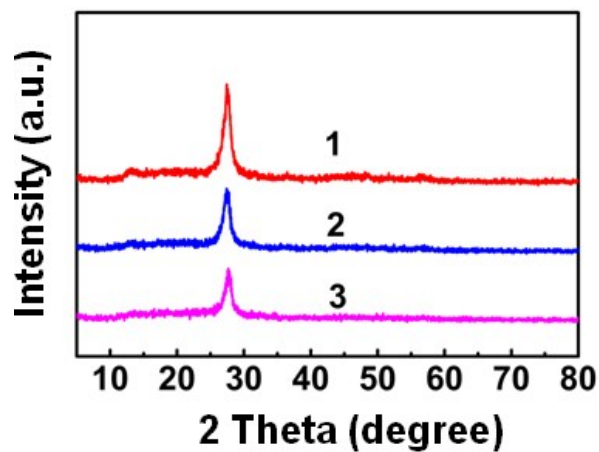


Fig. S9 XRD patterns of (1) Ni²⁺ doped CoP/g-C₃N₄-3, (2) Ni²⁺ doped CoP/g-C₃N₄-5, (3) Ni²⁺ doped CoP/g-C₃N₄-7.

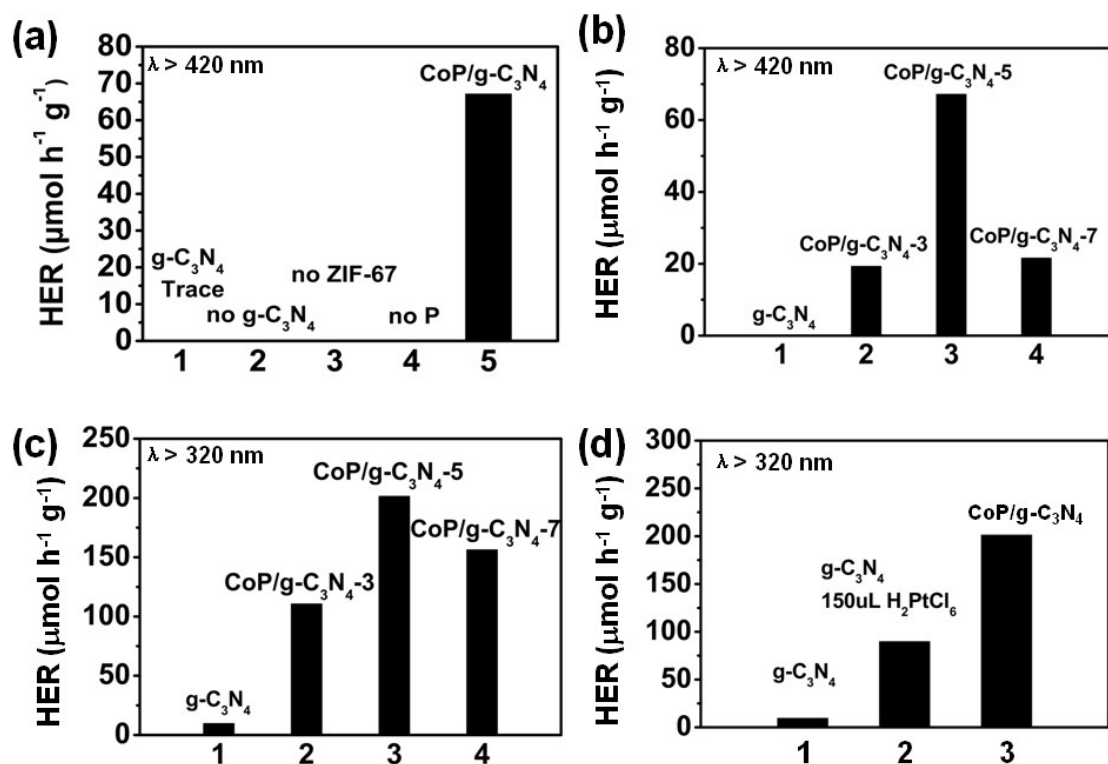


Fig. S10 Comparison of hydrogen production rate of different catalysts. (a) and (b) was under $\lambda > 420 \text{ nm}$. (c) and (d) was under $\lambda > 320 \text{ nm}$. The concentration of 150 mL H_2PtCl_6 aqueous solution is 0.0193 M. The corresponding amount of Pt photodeposited as cocatalyst was 2 wt%.

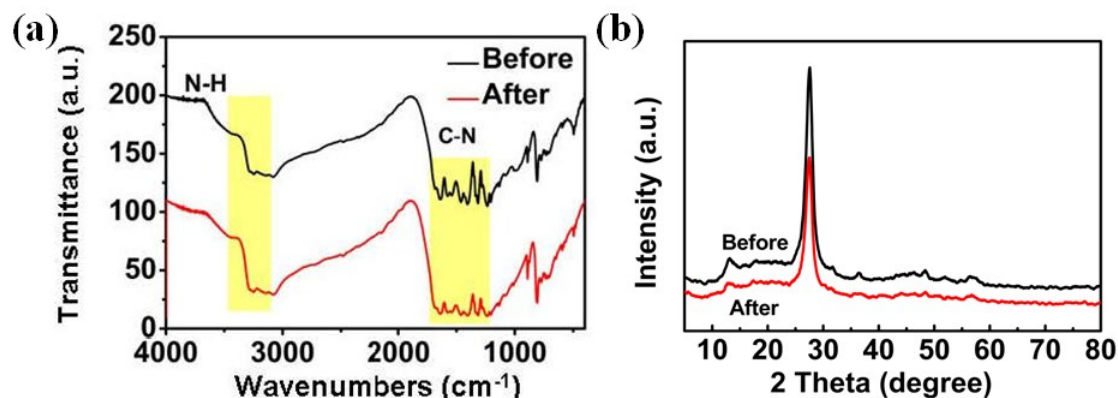


Fig.S11 FT-IR of $\text{CoP/g-C}_3\text{N}_4$ before and after photocatalysis.

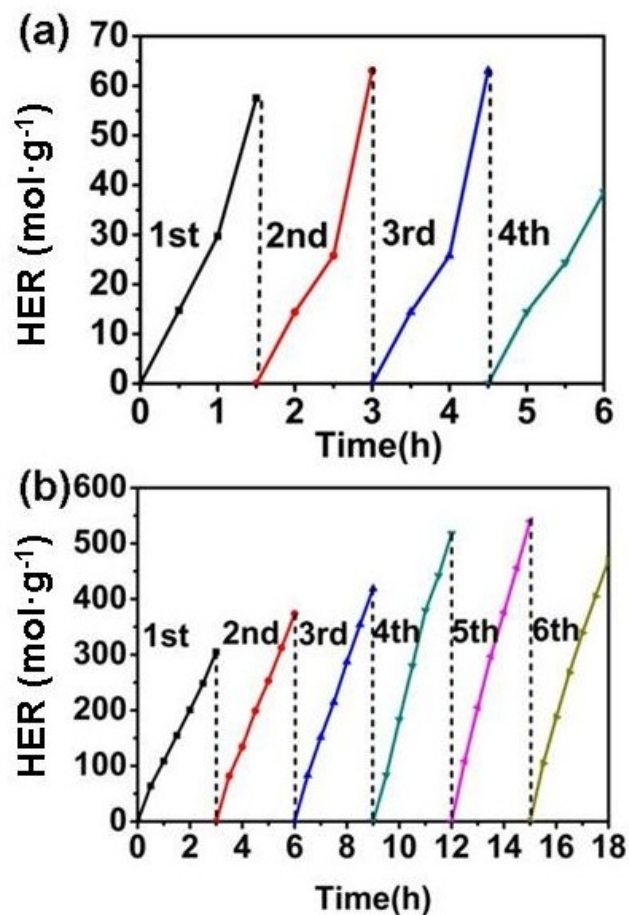


Fig.S12 Photocatalytic hydrogen production of 16 h over CoP/g-C₃N₄ with evacuation every 3 h.

This system contained 30 mg of the CoP/g-C₃N₄ photocatalyst and 50 mL of 20 vol% triethanolamine aqueous solution under (a) visible-light irradiation ($\lambda > 420$ nm) and (b) visible-light irradiation ($\lambda > 320$ nm), using 300 W Xe lamp as light source.

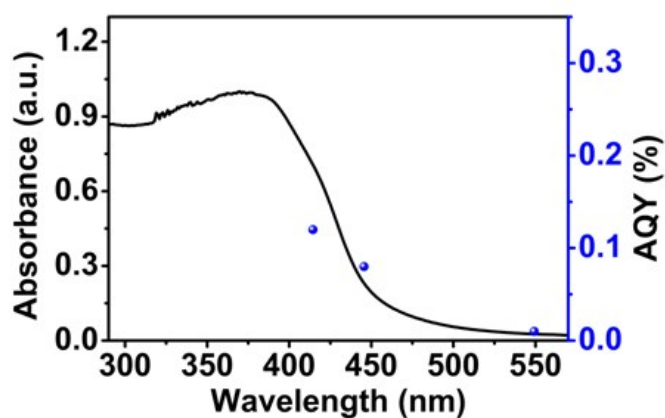


Fig.S13 UV-vis-diffuse reflectance spectrum and AQY of CoP/g-C₃N₄ along with light wavelength.

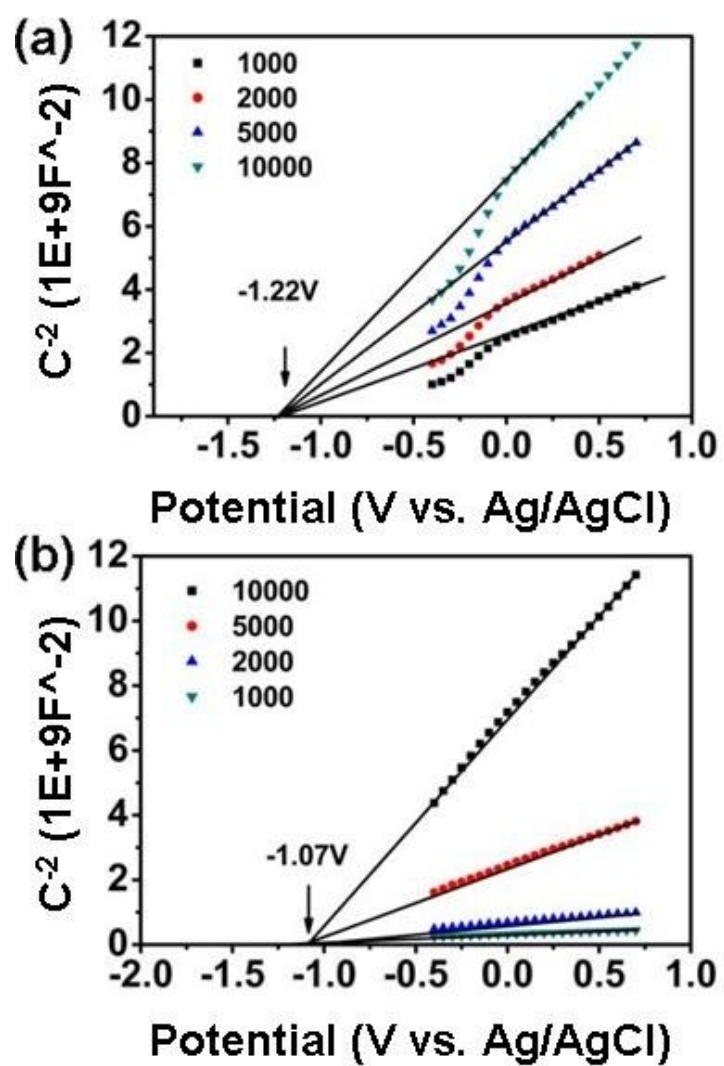


Fig.S14 Mott-Schottky plot of (a) g-C₃N₄, (b) CoP/g-C₃N₄-5 in 0.1 M Na₂SO₄ aqueous solution.

Table S1. Summary of various catalysts for photocatalytic H₂ evolution

Photocatalysts	sacrificial agent	Light source	Activity	Ref.
Pt/PtO ₂ /CoO _x /C ₃ N ₄	/	300 W Xe lamp (> 300 nm)	61 μmol g ⁻¹ h ⁻¹	[1]
UiO-66/g-C ₃ N ₄ /Pt	20 mL ascorbic acid solution (0.1 M)	300 W Xe lamp with a 420 nm cutoff filter	14.11 × 10 ⁻⁶ M h ⁻¹	[2]
CoS/mpg-CN	100 mL of TEOA (10 vol%)	300 W Xe lamp with a 420 nm cutoff filter	36.5 μmol h ⁻¹	[3]
g-C ₃ N ₄ /nanocarbon/ZnIn ₂ S ₄	80 mL of 0.35 M Na ₂ S and 0.25 M Na ₂ SO ₃	Four low power UV-LEDs (3W, 420 nm)	29.97 μmol h ⁻¹	[4]
CoP cluster/PCN	/	300 W Xe lamp	53.8 μmol g ⁻¹ h ⁻¹	[5]
CoP/g-C ₃ N ₄	50 mL of TEOA (20 vol%)	300 W Xe lamp	201.5 μmol g ⁻¹ h ⁻¹	This work

1. G. Zhang, Z. Lan, L. Lin, S. Lin and X. Wang, *Chem. Sci.*, 2016, **7**, 3062-3066.
2. R. Wang, L. Gu, J. Zhou, X. Liu, F. Teng, C. Li, Y. Shen and Y. Yuan, *Adv. Mater. Interfaces*, 2015, **2**, 1500037.
3. Y. Zhu, Y. Xu, Y. Hou, Z. Ding and X. Wang, *Int. J. Hydrogen Energy* 2014, **39**, 11873-11879.
4. F. Shi, L. Chen, M. Chen and D. Jiang, *Chem. Commun.*, 2015, **51**, 17144-17147.
5. L. W, C. L and C. W, *Angew. Chem. Int. Ed.*, 2017, **56**, 9312-9317.